Proceedings of the 8th World Congress on Civil, Structural, and Environmental Engineering (CSEE'23)
Lisbon, Portugal – March 29 – 31, 2023
Paper No. ICSECT 116
DOI: 10.11159/icsect23.116

Seismic Response Control of Benchmark Building using Semi-active Shape Memory Alloy based Tension Sling Damper

Sujata Mehta[1], Sharadkumar Purohit[2]
[1]Dr. B.N. College of Architecture
Karvenagar, Pune, Maharashtra, India
sujata.mehta@bnca.ac.in;
[2] Department of Civil Engineering, School of Engineering, Institute of Technology,
Nirma University, Ahmedabad, Gujarat, India
sharad.purohit@nirmauni.ac.in

Abstract – Seismic protection of building has remained important due to increased seismic activities as well as stringent seismic performance criteria. Recent past has seen surge in utilization of smart materials with controllable properties for seismic performance enhancement of structural systems. NiTinol Shape Memory Alloys (SMA) exhibiting super-elasticity and shape memory effect makes it a promising candidate for seismic protection applications. Novel SMA based tension sling damper (SMA-TSD) is developed incorporating super-elastic SMA slings and temperature controlled SMA springs. It is placed at ground story of a three story benchmark building for both; passive and semi-active seismic protection. Hysteretic behaviour of SMA-TSD is characterized by one-dimensional Tanaka model and is mapped to equivalent linear Voigt model for implementing it with linear benchmark building. Desired damper force of semi-active SMA-TSD is evaluated by Linear Quadratic Regulator (LQR) control strategy and realized by Shape Recovery Force (SRF) of SMA springs through SRF-Temperature-strain relationship. SRF is applied to expand passive hysteretic loop of super-elastic SMA slings within recoverable strain limit of 6%. Peak displacement, peak inter-story drift and peak acceleration responses show moderate reduction of the order ~12%-39% for passive off control strategy except peak acceleration at first story, substantial reduction of the order ~47%-71% when passive on and LQR control strategies are used for controlled benchmark building subjected to Taft seismic excitation. LQR control strategy yields substantial reduction in peak seismic parameters by realizing peak damper force in SMA-TSD as low as 284.90 N. Temperature is varied between practical range of 20^0C to 60^0C for generating SRF from SMA springs commanded by 5V battery only. Design parameters of SMA-TSD; diameter, number and length of SMA sling/s can be optimized to obtain enhanced seismic performance of the benchmark building.

Keywords**:** Semi-active damper**,** Linear Quadratic Regulator, Shape Memory Alloys, Benchmark building, Tanaka model

1. Introduction

Frequent occurrence of seismic activities warrants various seismic protection strategies. While passive seismic protection systems have been implemented successfully, active, semi-active and hybrid control systems, are evolving rapidly. Active control system requires continuous power supply during an earthquake, on the other hand semi-active systems show more promise with reduced power requirement. Semi-active devices developed till date, mostly utilize capabilities of smart materials to adjust their mechanical properties in real time by application of external power source such as voltage, current, magnetic field, electric field, temperature etc. Shape Memory Alloys (SMA), a relatively newer class of smart materials possess unique characteristics like super-elasticity and Shape Memory Effect (SME), along with suitable mechanical properties, making them a potential candidate for development of semi-active seismic protection device. A variety of SMAs (Cu-Zn, Cu-Al, Cu-Sn Fe-Pt, Fe-Mn- Si) are explored however, NiTi alloys are widely used SMAs for engineering applications [1]. NiTi SMA have found application in aeronautical, biomedical, robotic and automobile industries due to unique characteristics of; Shape Memory Effect (SME) - ability to regain original shape upon change in temperature and Super-elasticity - large elastic recoverable strain (of the order~6%). NiTi SMA exist in two phases namely austenite - stable at high temperature having body-centred cubic crystal structure and martensite - stable in low temperature having parallelogram structure. Phase transformation of SMA can be stress induced (loading and unloading) or temperature induced (heating and cooling). Nonlinear hysteretic behaviour of SMA was represented by one dimensional phenomenological model

by Tanaka [2] that defines total strain comprising of elastic strain, transformation strain and thermodynamic strain. The model provides set of equations for evolution of kinematics of martensite volume fraction for SMA. Graesser and Cozzarelli [3] have represented hysteretic behaviour of SMA founded on classic Bouc-Wen model, widely known as classical G-C model. This model is updated by Ren et al. [4] defining different parameters for loading and unloading branches.

Seelecke et al [5], Han et al [6] have implemented SMA wire bracings for seismic response control of steel frames by exploiting hysteretic damping and super-elastic properties of SMA. SMA based passive dampers were developed to control seismic response of RCC framed structures by Dolce et al [7] and McCormik et al [8], while for steel framed structures, by Mortazavi et al [9]. Implementation of pre-strained SMA based devices by Zhang and Zhu [10] revealed that pre-strained NiTi wires were more effective in controlling norm drift ratio and norm level acceleration of a building. Huang [11] has developed temperature controlled SMA based active Tuned Mass Damper (TMD) for seismic control of steel framed structure. Naeem et al [12] implemented hybrid SMA based energy dissipation device (SMA bar with passive slit damper) with seven story steel structure. Gur et al [13] have presented semi-active SMA based thermally modulated Friction Pendulum – tmSMA-FP, which shows enormous control efficiency for structures subjected to near-fault earthquakes.

Major objective of the present study is to develop novel semi-active Shape Memory Alloy based Tension Sling Damper (SMA-TSD), and implement it with three story benchmark building. Desired control force has been obtained by optimal control strategy, LQR and solving inverse problem of voltage-temperature- shape recovery force of semi-active SMA-TSD. Unified one-dimensional Tanaka model, being simple and versatile, is considered to represent nonlinear hysteretic behaviour of SMA slings. Linear Voigt model comprising of equivalent elastic stiffness and equivalent viscous damping components is used to map nonlinear hysteresis behaviour of SMA-TSD to implement it with linear benchmark building. Seismic performance of benchmark building fitted with semi-active SMA-TSD at ground story is evaluated in terms of peak responses; displacement, inter-story drift, acceleration and damper force under Taft seismic excitation.

2. Modelling and Mechanism of Semi-active SMA-TSD

Proposed semi-active SMA-TSD comprises of two major components, 1) SMA slings which utilize super-elastic property within maximum recoverable strain limit of 6% and 2) SMA springs which utilize Shape Memory Effect (SME) to improve damping capabilities. SMA slings are represented by unified Tanaka model expressing mechanical stress for isothermal loading/unloading process as,

$$\sigma = [E_A + \xi(E_M - E_A)]\,[\varepsilon - \xi H^{cur}(\sigma)] \tag{1}$$

where σ is applied stress, ε is total strain and $H^{cur}(\sigma)$ = maximum recoverable transformation strain in SMA, E_A = elastic modulus of austenite phase and E_M = elastic modulus of martensite phase of SMA. 'ξ' is percentage of martensite present in SMA by volume fraction. Martensite volume fraction (ξ) can be evaluated through Eq. (2) and Eq. (3).

$$\xi = 0 \text{ ; if } T \geq M_s^\sigma \text{ or } T \geq A_f^\sigma; \quad \xi = 1 \text{; if } T \leq M_f^\sigma \text{ or } T \leq A_s^\sigma \tag{2}$$

$$\xi = \frac{(M_s^\sigma - T)}{(Ms - Mf)}; \quad \text{if } M_f^\sigma < T < M_s^\sigma; \quad \xi = \frac{(A_f^\sigma - T)}{(A_f - A_s)} \text{ ; if } A_s^\sigma < T < A_f^\sigma \tag{3}$$

where T is ambient temperature, M_s and M_f are start and finish temperatures for martensite while A_s and A_f are start and finish temperatures of austenite phase of SMA which, in the presence of applied stress σ and stress influence co-efficient in austenite and martensite phase C_A and C_M, modifies to

$A_s^\sigma = A_s + \frac{\sigma}{C_A}$; $M_s^\sigma = M_s + \frac{\sigma}{C_M}$;

Nonlinear stress-strain behaviour depicted by set of equations, Eq. (1) to Eq. (3), offers difficulties when implemented with linear system since computationally intensive dynamic analysis becomes evident. However, various seismic codes permit modelling of nonlinear hysteretic behaviour with equivalent linear elastic stiffness and equivalent viscous damping co-efficient if later does not exceed by 30% of energy dissipation [14]. Few studies [15] have successfully converted nonlinear behaviour of SMA to linear equivalent elastic stiffness and equivalent viscous damping and implemented with linear system as shown in Figure 1(a). Therefore, in the present study damper force of SMA-TSD has been evaluated using linear Voigt model defined as,

$$F_{SMA}(t) = k_{eq}\, x(t) + c_{eq}\, \dot{x}(t) \tag{4}$$

where $x(t)$ and $\dot{x}(t)$, are input displacement and input velocity while k_{eq} is equivalent elastic stiffness expressed from Figure 1(a) as

$$k_{eq} = \frac{(F_{max} - F_{\min})}{(x_{max} - x_{min})} \tag{5}$$

and c_{eq} is equivalent viscous damping co-efficient derived from equivalent viscous damping ratio, ξ_{eq}, evaluated from energy dissipated by the system in one cycle given as,

$$\xi_{eq} = \frac{W_D}{2\,\Pi\, k_{eq}\, x_{max}^2} \tag{6}$$

where W_D is energy loss per cycle by the hysteretic semi-active SMA-TSD, ξ_{eq} is the equivalent viscous damping ratio, x_{max} is the maximum damper displacement amplitude. Using basic definition of viscous damping constant, equivalent viscous damping co-efficient , c_{eq}, can be obtained as,

$$c_{eq} = 2\,\xi_{eq}\,\sqrt{k_{eq} m} \tag{7}$$

where m represents mass of the story at the level of semi-active SMA-TSD.

While equivalent stiffness, k_{eq}, of Voigt model remains constant over the period of dynamic analysis, equivalent viscous damping co-efficient, c_{eq}, has been evaluated at each instance of time to simulate the physical phenomena of damping more practically.

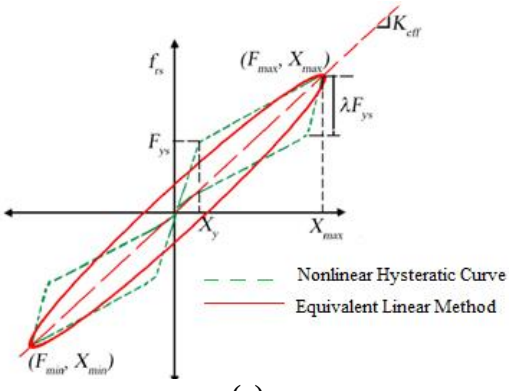

(a)

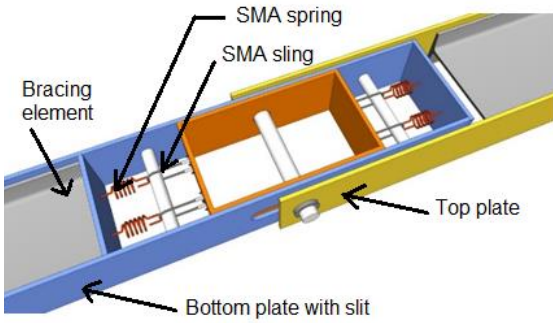

(b)

Figure 1: (a) Hysteresis curve of SMA NiTinol wire and equivalent linear model (Ghodke and Jangid, 2016), (b) 3D view of proposed semi-active SMA-TSD

Figure 1(b) shows 3D view of the proposed novel semi-active SMA-TSD, modified from passive SMA-TSD implemented with SDOF system [16]. Passive SMA-TSD when fitted with linear system under seismic inputs, offers damping due to strain induced in SMA slings which may be well below maximum recoverable strain and thus contributing limited damping increment to the system. Therefore, it is proposed to add temperature-controlled SMA springs which further extend SMA slings to maximum recoverable strain and thus exploit Shape Memory Effect (SME) of SMA springs to improve hysteresis loop of super-elastic SMA slings. SMA springs used in the present study are of extension type with martensite phase in their extended state, and tend to shrink when voltage is commanded.

Shape Recovery Force (SRF) produced in the SMA springs are shown in Figure 2(a) for right sway and Figure 2(b) for left sway position of SMA-TSD when subjected to input motion. The set of SMA slings subjected to tensile strain, shown in red colour, are stretched further by temperature activated SMA springs to produce desired recoverable strain as shown in Figure 2.

(a) (b)

Figure 2: Shape Recovery Force SRF in SMA springs of semi-active SMA-TSD (a) Right sway position (b) Left sway position

3. System Model

Building considered in the present study is a laboratory based three story modal building by Dyke et al [17], widely used to test efficacy of control devices developed by researchers, fitted with semi-active SMA-TSD at the ground story. Equation of motion of controlled modal building is given as,

$$M\ddot{x}(t) + C\,\dot{x}(t) + Kx(t) = Gf(t) - ML\ddot{x}_g(t) \tag{8}$$

where M = mass matrix, C = damping matrix, K = stiffness matrix, G = location of damper, $f(t)$ = damper force, L = influence vector depicting location of masses in the modal building associated with seismic ground excitation, $x(t)$, $\dot{x}$(t) and $\ddot{x}$(t) are displacement, velocity and acceleration vectors of the mass relative to the ground. Mass, stiffness and damping matrices are given by Eq. (9) as defined by Dyke et al., (1996).

$$M=\begin{bmatrix}98.3 & 0 & 0\\ 0 & 98.3 & 0\\ 0 & 0 & 98.3\end{bmatrix} kg; \qquad K=1\times 10^5\begin{bmatrix}12 & -6.84 & 0\\ -6.84 & 13.7 & -6.84\\ 0 & -6.84 & 6.84\end{bmatrix} N/m;$$

$$C=\begin{bmatrix}175 & -50 & 0\\ -50 & 100 & -50\\ 0 & -50 & 50\end{bmatrix} Ns/m; \quad f(t)=[F_{SMA}]; \qquad G=\begin{bmatrix}-1\\ 0\\ 0\end{bmatrix}; \quad L=\begin{bmatrix}1\\ 1\\ 1\end{bmatrix}; \tag{9}$$

Displacement degree of freedom $x = [x_1\ x_2\ x_3]^T$ associated with mass at each story, m_i, where i = 1,2,3. Damper force by semi-active SMA-TSD expressed as F_{SMA} is as defined in Eq. (4). Desired damper force for the benchmark building is determined by LQR control law which is realized by combination of strain in super-elastic SMA slings due to input motion and applying Shape Recovery Force (SRF) by temperature controlled SMA springs.

Design parameters of SMA spring; spring wire diameter, coil diameter and number of coils were derived such that desired force from LQR control law can be realized for most of the input motion. Spring wire diameter is considered 1 mm, coil diameter D is considered 3 mm to accommodate the minimum D/d ratio 3. SMA spring has material density $\rho = 6.45\times10^3$ kg/m^3, specific heat C = 465.2 J/ (kg °C), and convection heat transfer coefficient h = 131W/ (m^2 °C).

Performance Index, J, with weighing matrix Q for state variables and control effort R as defined in Eq. (10) is minimized. State weighing matrix, Q, is defined as [1 0 0 0 0 0; 0 1 0 0 0 0; 0 0 1 0 0 0; 0 0 0 0 1 0; 0 0 0 0 0 1] and control effort value R considered is 1 x 10^{-7}.

$$J = \int_0^t (z^T Q\, z + u^T R u)\, dt \tag{10}$$

where $z = [x \;\; \dot{x}]$ is state variable vector and u is external input. The semi-active SMA-TSD generates force due to strain produced in SMA-TSD due to temperature command given to SMA springs. However, implementation of LQR control law with benchmark building results into desired force to be generated through SMA-TSD. Thus, an inverse problem of Force-Strain- Temperature needs to be solved.

Temperature command on SMA springs result in to Shape Recovery Force (SRF) which assists in inducing additional strain in super-elastic SMA slings over and above the strain produced due to input motion. The SRF is expressed as,

$$SRF = G(T)\, d^4\, \delta\, /(8\, nD^3) \tag{11}$$

where $G(T)$ = shear modulus of SMA based on state of temperature-controlled phase transformation, d = diameter of spring wire, δ = deflection in spring, n = number of coils, D = diameter of spring coil.
Shear modulus of SMA spring can be calculated as shown in Eq. (12),

$$G(T) = G_M + (G_A - G_M)/2\, [1 + sin\, \phi\, (T - T_M)] \tag{12}$$

where $\phi = \pi/ (A_f - A_s)$, G_M and G_A are the shear moduli of martensite and austenite, respectively for $M_f \leq T \leq A_f$. Shear modulus of NiTi SMA is a function of temperature. For NiTi SMA, shear modulus in austenite phase (G_A) is higher than shear modulus in martensite phase (G_M). In the process of heating, T_M is given as shown in Eq. (13)

$$T_M = (A_s + A_f)/2 \tag{13}$$

To generate temperature T for obtaining desired value of $G(T)$, voltage applied to SMA springs can be calculated based on Eq. (14)

$$\text{Voltage} = (\text{Power}/\text{Resistance})^{1/2} \tag{14}$$

and Power $P = C\, V \frac{\rho(T - T_0)}{dt} + h\, A(T - T_0)$ where ρ = material density, C = specific heat, V = wire volume, h = convection heat transfer co-efficient, A = wire surface area, Resistance of SMA spring Rt, at any temperature is given by Song et al., (2011), is mentioned in Eq. (15)

$$Rt = R_{0M} + (T - T_{0M})\, \partial RM/\partial T + \sigma\, \partial RM/\partial s \tag{15}$$

where R_{0M} = Nominal wire resistance in martensite phase, T_{0M} = temperature at which the nominal resistances were measured, $\partial RM/\partial T$ = linear temperature dependence of martensite resistance, $\partial RM/\partial s$ = linear stress dependence of martensite resistance.

In order to assess the efficacy of semi-active SMA-TSD, two problems of passive damper; (i) Passive on control in which SMA springs are commanded with constant temperature of 60^0 C throughout the seismic input, (ii) Passive off control in which damper force is obtained passively, i.e., SMA-TSD without SMA springs; are solved.

4. Results and Discussion

Seismic response parameters of controlled benchmark building fitted with semi-active SMA-TSD at ground story are evaluated using three control strategies; (i) Passive off (ii) Passive on and (iii) Linear Quadratic Regulator (full state feedback) when subjected to Taft seismic excitation (1952). Following majority of literature, which consider strong motion type earthquakes to study seismic response control, present study focusses on controlled response of benchmark building subjected to Taft seismic excitation. The peculiarity of this seismic excitation is having predominant frequencies over significant period of time. However, controlled response of benchmark building with semi-active SMA-TSD subjected to pulse type and strong motion type seismic excitations have been studied [18]. Since benchmark building considered is a laboratory based scaled modal building, time scaled Taft seismic excitation is applied with PGA of 0.173g. Uncontrolled seismic response of benchmark building is determined and subsequently compared with seismic response of controlled benchmark building.

Table 1: Seismic response parameters of benchmark building for Taft seismic excitation

Seismic Response Parameters	Story Level	Control Strategy			
		Uncontrolled	Passive off	Passive on	LQR
Peak Displacement (cm)	1	0.209	0.128 (-38.76)	0.067 (-67.95)	0.059 (-71.78)
	2	0.321	0.204 (-36.45)	0.122 (-62.00)	0.110 (-65.74)
	3	0.380	0.264 (-30.53)	0.159 (-58.16)	0.144 (-62.11)
Peak Inter-story Drift (cm)	1	0.209	0.128 (-38.80)	0.067 (-67.95)	0.059 (-71.78)
	2	0.117	0.091 (-22.23)	0.062 (-47.01)	0.058 (-50.43)
	3	0.076	0.073 (-03.95)	0.037 (-51.32)	0.036 (-52.64)
Peak Acceleration (m/s^2)	1	4.244	4.921 (+16.00)	1.442 (-66.03)	1.380 (-67.49)
	2	4.419	3.872 (-12.38)	1.760 (-60.18)	1.648 (-62.71)
	3	5.290	5.090 (-03.79)	2.607 (-50.72)	2.515 (-52.46)
Peak Damper Force (N)			185.99	242.40	284.90

Table 1 summarizes peak response parameters; displacement, inter-story drift, acceleration and damper force of controlled benchmark building subjected to time scaled Taft seismic excitation. Diameter and length of SMA sling for the SMA-TSD was derived based on passive off control strategy and same are used for both, passive on and LQR, control strategies. SMA springs are designed to maintain minimum D/d ratio as mentioned in Section 3.

It is evident from Table 1 that passive off control strategy yields moderate reduction while passive on and LQR control strategies yield substantial reduction in peak displacement, peak inter-story drift and peak acceleration response for controlled benchmark building vis-à-vis uncontrolled response. Peak displacement response is found to reduce on and average by ~30%, 60% and 65% for passive off, passive on and LQR control strategies respectively across all the stories. Semi-active SMA-TSD yields reduction in peak inter-story drift response by 38.80%, 67.95% and 71.78% for passive off, passive on and LQR control strategies respectively; at the story where damper is fitted. While passive off control strategy yields marginal reduction in peak roof acceleration, passive on and LQR control strategies show reduction of 50.72% and 52.46%, respectively. Peak damper force realized by semi-active SMA-TSD is 185.99 N for passive off, 242.40 N for passive on and 284.90 N for LQR control strategies. Thus, SMA-TSD is found to effectively reduce peak response parameters for controlled benchmark building compared to uncontrolled response.

Figure 3(a), Figure 3(b) and Figure 3(c) depicts peak displacement, peak inter-story drift and peak acceleration variation across all stories of controlled benchmark building. It is clearly readable that LQR control strategy yields highest reduction in peak response parameters across all stories of the controlled benchmark building followed by passive on and passive off

control strategies. Damper force realized by semi-active SMA-TSD when fitted with benchmark building under Taft seismic excitation is shown in Figure 3(d).

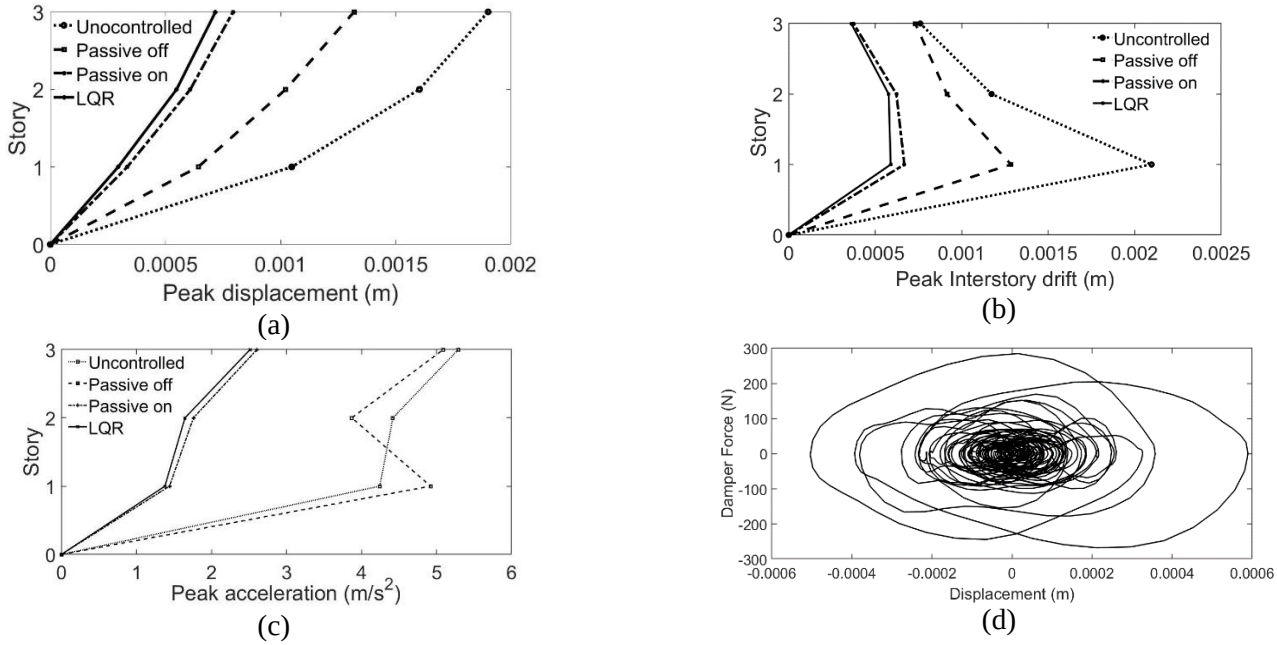

Figure 3: Peak seismic response parameters for three story benchmark building subjected to Taft seismic excitation; (a) Displacement, (b) Inter-story drift (c) Acceleration and (d) Damper force vs Displacement

Desired temperature evaluated by inverse relationship of Force-Strain- Temperature as discussed in Section 3 is plotted with time stamping in Figure 4(a). It is evident that SMA spring is commanded with temperature variation between 20^0 C to 60^0 C in order to produce maximum recoverable strain in super-elastic SMA slings. Since strain in SMA slings produced due to input motion is on low on receding end of the seismic excitation, semi-active SMA-TSD needs to be commanded more frequently. Time history plots of roof displacement and roof acceleration for controlled benchmark building subjected to Taft seismic excitation, evaluated by all three control strategies; passive off, passive on and LQR, are as shown in Figure 4(b) and Figure 4(c), respectively. Reduction in roof displacement and roof acceleration throughout the time history for controlled benchmark building as compared to the uncontrolled response is observed. Early occurrence of peak roof displacement and peak roof acceleration for controlled benchmark building vis-à-vis uncontrolled response is seen.

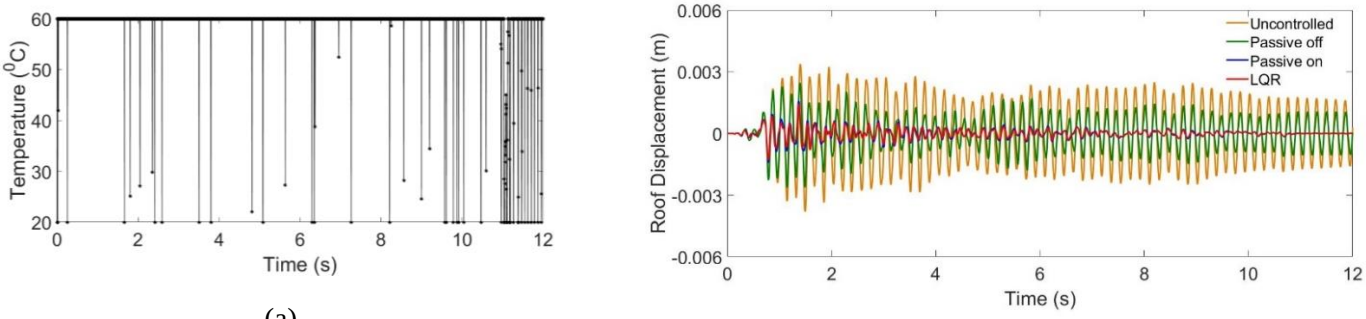

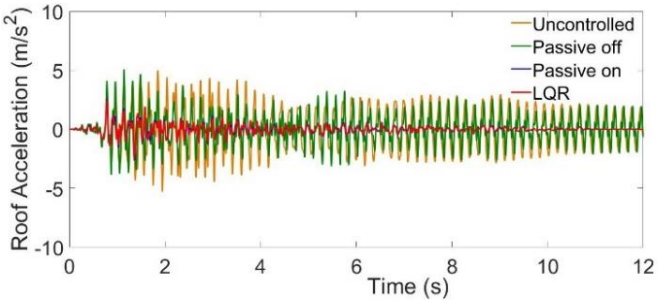

(c)

Figure 4: Time history plot for (a) Temperature variation in SMA spring (b) Roof displacement of benchmark building (c) Roof acceleration of benchmark building

5. Conclusion

Three story benchmark building fitted with semi-active SMA-TSD at ground story subjected to Taft seismic excitation is solved with three control strategies; passive off, passive on and LQR. Semi-active SMA-TSD is developed using super-elastic SMA slings and temperature controlled SMA springs. One dimensional Tanaka model is used to represent nonlinear hysteretic stress-strain relationship of SMA slings. Equivalent linear Voigt model is considered to map nonlinear hysteretic behaviour of SMA sling to implement semi-active SMA-TSD with linear benchmark building problem. State space representation is employed to represent dynamics of the controlled benchmark building and numerical algorithm of Runge-Kutta method is used for dynamic analysis. Seismic response parameters; peak displacement, peak inter-story drift and peak acceleration and peak damper force are evaluated for controlled benchmark building and are compared with uncontrolled response. Major conclusions derived from the present study are (i) proposed novel SMA-TSD is found to be effective in reducing peak seismic response parameters for the controlled benchmark building (ii) out of three control strategies; passive off, passive on and LQR, considered in the present study, LQR control strategy yields highest and substantial reduction in all peak response parameters of controlled benchmark building for Taft seismic excitations. (iii) passive on and LQR control strategies yield substantial reduction in peak seismic response parameters through SMA spring commanded by temperature range as low as 20^0 C to 60^0 C with a 5 V battery power source. Present paper outlines results of controlled response of benchmark building with SMA-TSD subjected to strong motion seismic excitations only.

References

[1] J. M. Jani, M. Leroy, A. Subik and M. Gibson, 2014. A Review of Shape Memory Alloy Research, Applications and Opportunities. Materials and Design, vol. 56, pp. 1078-1114.

[2] K. Tanaka, “A thermomechanical sketch of shape memory effect: one-dimensional tensile behaviour”, Research Mechanical, vol. 2, no. 3, pp. 59-72, 1986.

[3] E. Graesser and F. Cozzarelli, “Shape-Memory Alloys as new materials for seismic isolation”, Journal of Engineering Mechanics, vol. 117, no. 11, pp. 2590-2608, 1991.

[4] W. Ren, L. Hongnan and S. Gangbing, “A one-dimensional strain-rate-dependent constitutive model for super-elastic shape memory alloys”, Smart Materials and Structures, vol. 16, no. 1, pp. 191–197, 2007.

[5] S. Seelecke, O. Heintze and A. Masuda, “Simulation of earthquake-induced structural vibrations in systems with SMA damping element”. Proceedings of the SPIE Smart Structures & Materials, San Diego, USA, 4697: pp. 1-8, 2002.

[6] Y. Han, Q. S. Li, A. Li, A.Y.T. Leung and P. Lins, “Structural vibration control by shape memory alloy damper”, Earthquake Engineering and Structural Dynamics, vol. 32, no. 3, pp. 483–494, 2003.

[7] M. Dolce, D. Cardone, F. Ponzo and C. Valente, “Shaking table tests on reinforced concrete frames without and with passive control systems”, Earthquake Engineering and Structural Dynamics, vol. 34, no. 14, pp. 1687–1717, 2005.

[8] J. McCormik, R. DesRoches, D. Fugazza and F. Auricchio, “Seismic vibration control using super-elastic shape memory alloys”, Journal of Engineering Materials and Technology, vol. 128, no. 3, pp. 294-301, 2006.

[9] S.M.R. Mortazavi, M. Ghassemieh and S. A. Motahari, “Seismic control of steel structures with shape memory alloys”, International Journal of Automation and Control Engineering, vol. 2, no. 1, pp. 28-34, 2013.

[10] Y. Zhang and S. Zhu, “Seismic response control of building structures with super-elastic Shape Memory Alloy Wire dampers”, Journal of Engineering Mechanics, vol. 134, no. 3, pp. 240-251, 2008.
[11] H. Huang, K. M. Mosalam and W. Chang, “Adaptive tuned mass damper with shape memory alloy for seismic application”, Engineering Structures, vol. 223, no. 15, pp. 111-171, 2020.
[12] A. Naeem, M. N. Eldin and J. Kim, “Seismic performance evaluation of a structure retrofitted using steel slit dampers with shape memory alloy bars”, International Journal of Steel Structures, vol. 17, no. 4, pp. 1627–1638, 2017.
[13] S. Gur, G. N. Frantziskonis and S. Mishra, “Thermally modulated shape memory alloy friction pendulum (tmSMA-FP) for substantial near-fault earthquake structure protection”, Structural Control and Health Monitoring, vol. 24, no. 11, 2017.
[14] American Association of State Highway and Transportation Officials, “Guide specifications for seismic isolation design – 4th edition”, Washington D.C., USA, 2014.
[15] S. Ghodke and R. S. Jangid, “Equivalent linear elastic-viscous model of shape memory alloy for isolated structures. Advances in Engineering Software, vol. 99, no. 22, pp. 1-8, 2016.
[16] S. H. Mehta and S. P. Purohit, “Proposed SMA Tension Sling Damper for Passive Seismic Control of Building”, Electronic Journal of Structural Engineering, vol. 19, pp. 49–59, 2019.
[17] S. J. Dyke, B. F. Spencer Jr., M. K. Sain and J. D. Carlson, “Modelling and control of magnetorheological dampers for seismic response reduction”, Smart Materials and structures, vol. 5, no. 5, pp. 565-575, 1996.
[18] S. H. Mehta “A Novel SMA Damper for Enhanced Seismic Response of Structural Systems: Some Investigations”, Ph. D. Dissertation, Nirma University, India, 2021.